

# Continual Adversarial Defense

Qian Wang<sup>1</sup>, Yaoyao Liu<sup>2</sup>, Hefei Ling<sup>1\*</sup>, Yingwei Li<sup>2</sup>, Qihao Liu<sup>2</sup>, Ping Li<sup>1</sup>,  
Jiazong Chen<sup>1</sup>, Alan Yuille<sup>2</sup>, and Ning Yu<sup>3\*</sup>

<sup>1</sup> Huazhong University of Science and Technology, China  
{yqwq1996, lhefei, lpshome, jzchen}@hust.edu.cn

<sup>2</sup> Johns Hopkins University, USA

{yliu538, yingwei.li, qliu45, ayuille1}@jhu.edu

<sup>3</sup> Salesforce Research, USA ning.yu@salesforce.com

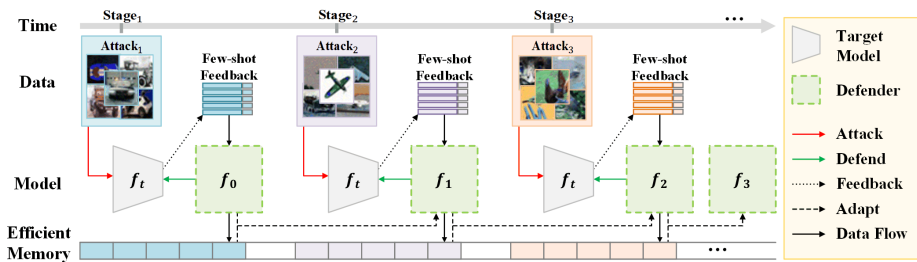


**Fig. 1:** In a dynamic environment, the target model  $f_t$  encounters a wide spectrum of attacks across various stages while being safeguarded by the defender. During the  $i$ -th stage, the defender leverages few-shot defense feedback, which is collected by the online defense system or provided by the security department and users of the target model, to adapt to emerging threats. Furthermore, the defender is required to efficiently manage memory utilization to store the cache, preserving insights gained from past attacks.

**Abstract.** In response to the rapidly evolving nature of adversarial attacks against visual classifiers on a monthly basis, numerous defenses have been proposed to generalize against as many known attacks as possible. However, designing a defense method that generalizes to all types of attacks is not realistic because the environment in which defense systems operate is dynamic and comprises various unique attacks that emerge as time goes on. The defense system must gather online few-shot defense feedback to promptly enhance itself, leveraging efficient memory utilization. Therefore, we propose the first continual adversarial defense (CAD) framework that adapts to any attacks in a dynamic scenario, where various attacks emerge stage by stage. In practice, CAD is modeled under four principles: (1) continual adaptation to new attacks without catastrophic forgetting, (2) few-shot adaptation, (3) memory-efficient adaptation, and (4) high accuracy on both clean and adversarial images. We explore and integrate cutting-edge continual learning, few-shot learning, and ensemble learning techniques to qualify the principles. Experiments conducted on CIFAR-10 and ImageNet-100 validate the effectiveness of our approach against multiple stages of modern adversarial

\* Corresponding authors

attacks and demonstrate significant improvements over numerous baseline methods. In particular, CAD is capable of quickly adapting with minimal feedback and a low cost of defense failure, while maintaining good performance against previous attacks. Our research sheds light on a brand-new paradigm for continual defense adaptation against dynamic and evolving attacks.

**Keywords:** Adversarial Defense · Continual Learning

## 1 Introduction

In recent years, deep neural networks have been widely used in numerous vision tasks [29], leading to remarkable breakthroughs. However, many neural networks are vulnerable to adversarial attacks, which aim to deceive a classifier by adding subtle perturbations to input images, thus altering prediction results. This vulnerability seriously jeopardizes the reliability of deep neural networks, particularly in security- and trust-sensitive domains.

Researchers have proposed various general defense methods against adversarial attacks. As a standard defense method, adversarial training [44] aims to enhance the robustness of the target model by training it with adversarial examples. Another branch of adversarial defense involves purifying the data stream [41] to remove potential adversarial perturbations or noise that could deceive the model. However, models of adversarial training often exhibit reduced classification accuracy on adversarial examples and may sacrifice classification capacity on clean images. On the other hand, purification techniques may appear more reliable, but the denoising procedure can inadvertently smooth the high-frequency texture of clean images, potentially causing issues for the target model.

From an application perspective, it is not realistic to design a defense method that can generalize to all types of attacks, including unseen ones. The truth is that the increasing number of defense strategies naturally stimulates the development of new attack algorithms [32]. As a result, the defense system encounters a dynamic environment characterized by numerous unique attacks with higher success rates in both white-box and black-box settings [20]. The target model is threatened by many attackers with various attacks, just like the defense scenario against Deepfake [13].

Inspired by online learning, the crucial approach to addressing dynamic scenarios lies in embracing a perpetually evolving defense strategy. Consequently, deploying a defense system on the cloud that continuously gathers attack examples from newly emerged adversarial algorithms and promptly adapts to these attacks represents a promising method for responding to such scenarios. As depicted in Fig. 1, a variety of attacks are detected across different stages, with the defender adapting to emerging threats by utilizing few-shot defense feedback. In this paper, we employ adversarial examples with ground truths as the defense feedback, sourced either from the online defense system’s crawling efforts or provided by the security department and users of the target model in real-world scenarios. The defender undergoes training with an initial attack and shares the

same training data and architecture as the target model. Meanwhile, attacks are initiated under the gray-box setting, wherein they possess knowledge of the classifier’s architecture and have access to training data, but remain unaware of the defense mechanism implemented.

Taking real-world considerations into account, we propose four principles for the scenario: (1) *Continual adaptation to new attacks without catastrophic forgetting*. As defenders, it is crucial to adeptly adapt to a multitude of new attacks occurring at different stages while preserving knowledge gained from previous encounters. (2) *Few-shot adaptation*. The escalation in feedback signifies a greater potential for attacks on the target model. Therefore, we cannot tolerate an excessive number of attacks before adaptation. (3) *Memory-efficient adaptation*. Over time, a continuous influx of attacks leads to the accumulation of defense feedback, potentially posing memory constraints. In practical terms, we may not have sufficient memory capacity to withstand this pressure. (4) *High accuracy in classifying both clean and adversarial images*. A robust defense should not compromise the interests of those it protects. Hence, ensuring high classification accuracy on both clean and adversarial images is paramount.

In this paper, we propose the Continual Adversarial Defense (CAD) framework, which aims to defend against evolving attacks in a stage-by-stage manner using few-shot defense feedback and efficient memory. In the first stage, we train an initial defense model using adversarial images from the initial attack. This model is specifically designed to classify images with adversarial noise, complementing the target model. Drawing inspiration from continual learning (CL), we expand the classification layer to adapt to the new attack as incremental classes. We then fine-tune this expanded layer using few-shot defense feedback. To address the over-fitting issue that arises from the few-shot fine-tuning process, we reserve embedding space in the defense model for future attacks. This is achieved by generating and assigning virtual prototypes, which help compress the embedding of previous attacks. To optimize memory usage in the data domain, we employ prototype augmentation which allows us to maintain the decision boundary of previous stages without the need to store any feedback explicitly. Simultaneously, we utilize a small model to ensemble the defense model with the target model by estimating reliable logits for input images, ensuring maximum classification accuracy for both clean and adversarial images.

Based on our comprehensive experiments conducted on CIFAR-10 and ImageNet-100, the CAD framework demonstrates strong performance in defending against multi-stage attacks relying on few-shot feedback while maintaining high accuracy on clean images. Our main contributions can be summarized as follows:

- To withstand the rapidly evolving adversarial attacks targeting image classifiers, we introduce, for the first time, a dynamic scenario featuring diverse attacks emerging at different stages to continuously enhance the defense. The defender must adeptly adapt to novel attacks using few-shot defense feedback and efficient memory management, while also retaining knowledge of past attacks and maintaining high performance on both clean and adversarial images.

- We propose the Continual Adversarial Defense (CAD) framework that defends against attacks in the dynamic scenario under four practical principles: continual adaptation without catastrophic forgetting, few-shot adaptation, memory-efficient adaptation, and high accuracy in classifying both clean and adversarial images. We leverage cutting-edge techniques including continual learning, few-shot learning, non-exemplar class incremental learning, and ensemble learning to satisfy the principles.

- Extensive experiments on CIFAR-10 and ImageNet-100 validate the effectiveness of CAD against multiple stages of 10 modern adversarial attacks using few-shot feedback and efficient memory and demonstrate significant improvements over 10 baseline methods.

## 2 Related Work

### 2.1 Adversarial Attacks

Adversarial attacks [9] attempt to fool a classifier into changing prediction results by attaching subtle perturbations to the input images while maintaining imperceptibility from human eyes. PGD [23] and BIM [18] generate adversarial examples through several iterations of perturbation and get significantly improved attack performance. DIM [40], TIM [7], and SIM [21] improve the transferability under the black-box setting and breach several defense techniques. Incorporating variance tuning, VIM [38] achieves a high attack rate against multiple advanced defense methods. In this paper, a wide spectrum of attacks is used to offense the target model at different stages under the gray-box setting.

### 2.2 Adversarial Defense

Adversarial training [23, 45] is the mainstream of adversarial defense that uses attacked samples to train a robust model. TRADES [44] characterize the trade-off between accuracy and robustness for classification problems via decomposing the robust error as the sum of the natural error and the boundary error. JEM [10] uses energy-based training of the joint distribution and improves the calibration and robustness of target models. Replacing the denoising diffusion probabilistic model with the elucidating diffusion model, DMAT [39] improves adversarial training and achieves new SOTA robust accuracy.

Another technical solution for protecting DNNs from adversarial attacks is adversarial purification [12, 28], which aims to purify the data stream before feeding it into the target model, functioning under the gray-box setting [32]. Based on an EBM trained with Denoising Score-Matching, Yoon et al. [41] propose Adaptive Denoising Purification (ADP) which conducts purification in a randomized purification scheme. Nie et al. [26] propose DiffPure that uses the forward and reverse processes of diffusion models to purify adversarial images.

Indeed, both adversarial training and purification methods have exhibited limitations in robustness, resulting in diminished classification performance on

clean images. Moreover, the dynamic environment introduces a multitude of unique attacks, rendering a single defense inadequate. In this paper, we present the Continual Adversarial Defense (CAD) framework as a solution to effectively counter various attacks emerging stage by stage, while ensuring robust performance in classifying clean images.

### 2.3 Continual Learning

Continual learning (CL) [22, 27] aims to learn from a sequence of new classes without forgetting old ones and attracts much attention to various computer vision tasks. Many works have been proposed for CL: by introducing different knowledge distillation (KD) losses to consolidate previous knowledge [27], by preserving a small number of old class data (exemplars) or augmented data (Zhu et al., 2021) to recall the old class knowledge [49], and by expanding the network capacity for new class data or freezing partial network parameters to keep the old class knowledge [47]. In recent years, some methods have aimed to solve the CL problem without depending on preserving data (called none-exemplar) [51], and some methods have attempted to learn new classes in a few-shot scenario [43] in which only a small number of new class data is gainable. In this paper, we convert the proposed defense scenario into a few-shot and non-exemplar CL setting, which necessitates the defense mechanism to utilize few-shot defense feedback and efficient memory for adaptation.

## 3 Threat Model and Defense Principles

The defense system is deployed online and functions within a dynamic environment marked by a plethora of unique attacks, driven by the proliferation of defenses that naturally prompt the development of new attack algorithms. As time progresses, numerous new attacks, accompanied by attack examples, will emerge on the internet, aiming to exploit vulnerabilities in the defense system and achieve breakthroughs. In response to this reality, we simulate the dynamic environment and propose a practical threat model. In this model, distinct attacks are identified across various stages, requiring the defender to adapt to evolving threats through the utilization of defense feedback. Typically, defense feedback is obtained through crawling efforts of the online defense system or is provided by security services and users of the target model. This feedback is crucial as it informs and influences the defender’s response to emerging threats, often discovered during screening or cleanup efforts in the real world. In this paper, we use adversarial examples with ground truths as the defense feedback. We formulate this attack vs defense scenario as follows.

Our scenario is established on the  $N$ -way  $K$ -shot classification paradigm. Attacks are launched under the gray-box setting [32] in which the attacks know the architecture of the target model  $f_t : \mathcal{X} \rightarrow \mathbb{R}^N$  which trained on  $\mathcal{D}_{\text{train}}$  and evaluated on  $\mathcal{D}_{\text{test}}$ , but blind to the defense, where  $\mathcal{X}$  is the image space.

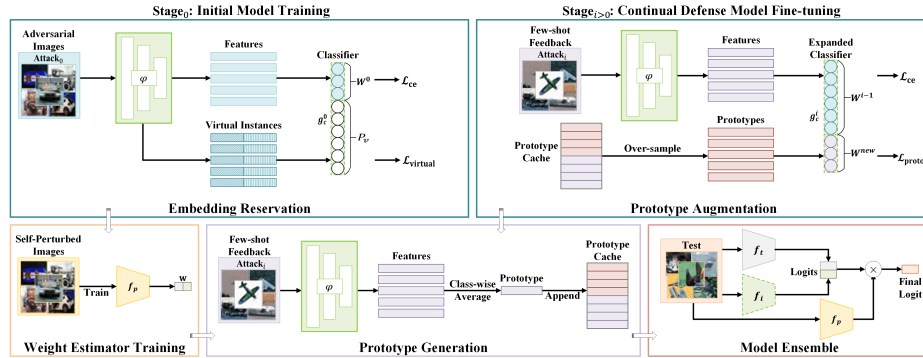


**Fig. 2:** Illustration of CAD. Regarding the classes with new attacks as incremental classes, we use continual adaptation to protect the target model while preventing catastrophic forgetting. In the 0-th stage, we reserve the embedding space for future attacks during training of the initial defense model  $f_0$  to alleviate overfitting brought by future fine-tuning. Then, a weight estimator model  $f_p$  is trained for model ensemble. In the  $i$ -th stage ( $i > 0$ ), we freeze the feature extractor  $\varphi$  of defense model  $f_i$  and fine-tune the expanded classifier  $g_c^i$  using few-shot defense feedback. To efficiently use memory, we store class-wise prototypes in the prototype cache at each stage and use them in the fine-tuning process. After all, the target model  $f_i$  and the scalable defense model  $f_i$  are ensembled by the weight estimator model  $f_p$  to maintain high accuracy in classifying clean and adversarial images.

The defender is permitted to visit  $\mathcal{D}_{train}$  and has the full knowledge of the initial attack  $A_0(\cdot)$  at the 0-th stage. At the  $i$ -th stage, where  $i = 1, 2, \dots, T$ , a new attack  $A_i(\cdot)$  is detected and the defender receives a set of feedback  $\mathcal{A}_{train}^i = \{(\mathbf{x}_{adv}^i, y) | \mathbf{x}_{adv}^i = A_i(\mathbf{x}), (\mathbf{x}, y) \in \mathcal{D}_{train}\}$  containing  $N \times K$  samples (i.e.,  $K$  samples for each of  $N$  classes) and uses it to adapt to the new attack. Evaluations are conducted on  $\mathcal{D}_{test}$  and  $\{\mathcal{A}_{test}^k\}_{k=0,1,\dots,i}$  at each stage  $i$ , where  $\mathcal{A}_{test}^i = \{(\mathbf{x}_{adv}^i, y) | \mathbf{x}_{adv}^i = A_i(\mathbf{x}), (\mathbf{x}, y) \in \mathcal{D}_{test}\}$ .

Taking reality into account, the defense mechanism should satisfy the following principles:

**Principle 1** *Continual adaptation to new attacks without catastrophic forgetting.*

In the dynamic environment, various new attacks will emerge on the internet as time goes on. Therefore, the defense mechanism must be capable of adapting to a range of new attacks across different time stages while also retaining knowledge of previous ones.

**Principle 2** *Few-shot adaptation.*

The increase in defense feedback directly correlates with the frequency of successful attacks on the target model. As defenders, we must proactively adapt the defense based on few-shot feedback to prevent potential security disasters that could arise from delayed action following an abundance of feedback.

**Principle 3** *Memory-efficient adaptation.*

Over time, the ongoing influx of attacks results in accumulating defense feedback, potentially leading to memory constraints. In practical terms, the defender may not have sufficient memory space to accommodate this accumulation. Consequently, storing all received defense feedback for adaptation is impractical and should be avoided.

**Principle 4** *High accuracy in classifying both clean and adversarial images.*

The previous defense strategies have led to a sacrifice in the classification accuracy of clean images, resulting in performance degradation. This decline could potentially hurt crucial real-world business operations. As a result, a defender must prioritize maintaining performance on both clean and adversarial images.

## 4 Continual Adversarial Defense Framework

As shown in Fig. 2, Continual Adversarial Defense (CAD) consists of continual adaptation to defend the target model while preventing catastrophic forgetting (Sec. 4.1), embedding reservation to alleviate overfitting brought by the few-shot feedback (Sec. 4.2), prototype augmentation for memory efficiency (Sec. 4.3), and model ensemble to ensure the classification performance on both clean and adversarial images (Section 4.4).

### 4.1 Continual Adaptation to New Attacks

In response to Principle 1, we use continual adaptation to defend against new attacks while preventing catastrophic forgetting. In the 0-th stage, an initial defense model  $f_0 : \mathcal{X} \rightarrow \mathbb{R}^N$  which consists of a feature extractor  $\varphi : \mathcal{X} \rightarrow \mathbb{R}^d$  and a classifier  $g_c^0 : \mathbb{R}^d \rightarrow \mathbb{R}^N$  is optimized under the full supervision using adversarial dataset  $\mathcal{A}_{\text{train}}^0 = \{(\mathbf{x}_{\text{adv}}^0, y) | \mathbf{x}_{\text{adv}}^0 = A_0(\mathbf{x}), (\mathbf{x}, y) \in \mathcal{D}_{\text{train}}\}$ . The defense model is designed to tackle adversarial examples, complementing the target model. In the  $i$ -th stage, the defense model  $f_i : \mathcal{X} \rightarrow \mathbb{R}^N$  adapts to new attack using defense feedback  $\mathcal{A}_{\text{train}}^i$ . Inspired by continual learning (CL) [27], we regard classes with the new attack as incremental classes and endow the defense model with scalability by classifier expansion.

Following [22], we expand the classifier from  $g_c^0 : \mathbb{R}^d \rightarrow \mathbb{R}^N$  to  $g_c^1 : \mathbb{R}^d \rightarrow \mathbb{R}^{N \times 2}$  in the first stage, and expand the classifier  $g_c^i$  from  $\mathbb{R}^d \rightarrow \mathbb{R}^{N \times i}$  to  $\mathbb{R}^d \rightarrow \mathbb{R}^{N \times (i+1)}$  in the  $i$ -th stage. The parameter of the expanded classifier is composed of the parameter of the old classifier and the newly initialized parameter:  $W^i = [W^{i-1}, W^{\text{new}}]$ , where  $W^i = [\mathbf{w}_1^i, \dots, \mathbf{w}_{N_i}^i]$  is the parameter matrix of  $g_c^i$  and  $N_i = N \times (i+1)$  is number of classes in stage  $i$  after expansion. Meanwhile, the ground truth of  $\mathcal{A}_{\text{train}}^i$  is rewritten corresponding to the incremental classes with the new attack <sup>4</sup>:

$$y^i = y + N \times i. \quad (1)$$

<sup>4</sup> We omit the networks' parameter in formulas

The initial defense model  $f_0$  will be trained in Sec. 4.2. After this, we freeze the feature extractor  $\varphi$  and fine-tune the part of the classifier expanded for the new attack  $A_i$  using few-shot feedback  $\mathcal{A}_{\text{train}}^i$  in Sec. 4.3.

For evaluation, we are just focusing on which class the image is placed in rather than being threatened by which attack. Thus the prediction for an instance  $\mathbf{x}$  is:

$$y_{\text{pred}} = (\arg \max f_i(\mathbf{x})) \% N \quad (2)$$

## 4.2 Embedding Reservation for Few-Shot Adaptation

A problem brought by the few-shot feedback in Principle 2 is over-fitting which is common in few-shot learning [30]. To tackle this issue, we choose to reserve embedding space for future attacks by generating and assigning virtual prototypes, squeezing the embedding space of previous attacks.

First, before training the defense model  $f_0$  at the 0-th stage, several virtual prototypes  $P_v = [\mathbf{p}_v^1, \dots, \mathbf{p}_v^V] \in \mathbb{R}^{d \times V}$  are pre-assign in the classifier and treated as "virtual classes" [43], where  $V = N \times T$  is the number of virtual classes, i.e. the reserved classes for future attacks. Therefore the output of current model is  $f_0(\mathbf{x}) = [W^0, P_v]^\top \varphi(\mathbf{x})$ .

Second, virtual instances are constructed by manifold mixup [35]:

$$\mathbf{z} = h_2(\lambda h_1(\mathbf{x}_{\text{adv},r}^0) + (1 - \lambda)h_1(\mathbf{x}_{\text{adv},s}^0)), \quad (3)$$

where  $\mathbf{x}_{\text{adv},r}$  and  $\mathbf{x}_{\text{adv},s}$  belong to different classes  $r$  and  $s$ , and  $\lambda \sim B(\alpha, \beta)$  is a trade-off parameter the same as [47].  $h_1$  and  $h_2$  are decoupled hidden layers of feature extractor i.e.  $\varphi(\mathbf{x}) = h_2 \circ h_1(\mathbf{x})$ .

Third, the embedding space reserving is conducted by training  $f_0$  with the following loss:

$$\begin{aligned} \mathcal{L}_v = & F_{\text{ce}}(\text{Mask}(f_0(\mathbf{x}_{\text{adv}}^0), y^0), \hat{y}) + F_{\text{ce}}(f_0(\mathbf{z}), \hat{y}) + \\ & + F_{\text{ce}}(\text{Mask}(f_0(\mathbf{z}), \hat{y}), \hat{\hat{y}}). \end{aligned} \quad (4)$$

where  $\hat{y} = \arg \max_j \mathbf{p}_v^{j\top} \varphi(\mathbf{x}_{\text{adv}}^0) + N$  is the virtual class with maximum logit, acting as the pseudo label.  $\hat{\hat{y}} = \arg \max_k \mathbf{w}_k^{0\top} \mathbf{z}$  is the pseudo label among current known classes.  $\gamma$  is a trade-off parameter,  $F_{\text{ce}}$  represents the standard cross-entropy loss [46], and function  $\text{Mask}(\cdot)$  masks out the logit corresponding to the ground-truth:

$$\text{Mask}(f_0(\mathbf{x}_{\text{adv}}^0), y^0) = f_0(\mathbf{x}_{\text{adv}}^0) \otimes (\mathbf{1} - \text{onehot}(y^0)) \quad (5)$$

where  $\otimes$  is Hadamard product and  $\mathbf{1}$  is an all-ones vector. The final loss for training the initial defense model is:

$$\mathcal{L}_{\text{ce}} = F_{\text{ce}}(f_0(\mathbf{x}_{\text{adv}}^0), y^0), \quad \mathcal{L}_0 = \mathcal{L}_{\text{ce}} + \gamma \mathcal{L}_{\text{virtual}} \quad (6)$$

In Eq. (4), it forces an instance to be away from the reserved virtual classes (item 1) and pushes the mixed instance towards a virtual class (item 2) and away



from other classes (item 3). Trained with  $\mathcal{L}_0$ , the embedding of initial benign classes will be more compact, and the embedding spaces for virtual classes will be reserved [47]. The reserved space allows the defense model to be adapted more easily in the future and alleviates overfitting brought by few-shot feedback.

### 4.3 Prototype Augmentation for Memory Efficiency

In response to Principle 3, we use prototype augmentation to efficiently manage memory.

When learning new classes, the decision boundary for previous classes can be dramatically changed, and the unified classifier is severely biased [50]. Many CL methods store a fraction of old data to jointly train the model with current data to address this issue [27]. However, preserving old feedback may also lead to memory shortage. For memory efficiency, we adopt prototype augmentation [51] to maintain the decision boundary of previous stages, without saving any feedback. We memorize one prototype in the deep feature space for each class with each attack, and over-sample (i.e.,  $U_B$ ) prototypes  $\mathbf{p}_B$  and ground-truths  $y_B$  to the batch size, achieving the calibration of the classifier:

$$\mathbf{p}_B = U_B(P_e), \mathcal{L}_{\text{proto}} = F_{\text{ce}}(\mathbf{p}_B, y_B) \quad (7)$$

where  $P_e = \{\mathbf{p}_e^j\}_{j=0}^{N \times i}$  is the set of class-wise average embedding (i.e., prototype cache) generated by feature extractor  $f_e^i$  the same as ProtoNet [30]:

$$\mathbf{p}_e^j = \frac{1}{K} \sum_{k=1}^K \mathbb{I}(y_k^i = j) \varphi(\mathbf{x}_{\text{adv},k}^i) \quad (8)$$

where  $\mathbb{I}(\cdot)$  is the indicator function, and  $K$  is the amount of feedback for each class.

In each stage, the defense model is adapted using the following loss:

$$\mathcal{L}_{\text{ce}} = F_{\text{ce}}(f_i(\mathbf{x}_{\text{adv}}^i), y^i), \quad \mathcal{L}_f = \mathcal{L}_{\text{ce}} + \mathcal{L}_{\text{proto}} \quad (9)$$

### 4.4 Model Ensemble for Clean and Adversarial Image Classification

To maintain high classification accuracy on both clean and adversarial images mentioned in Principle 4, we propose the model ensemble as the last part of CAD. Ensemble adversarial training (EAT) [34] which trains a robust model using adversarial samples generated by the target model is a simple yet effective way to defend against adversarial attack under the gray-box setting while maintaining the classification performance of clean images. We extend EAT to our scenario by training a small weight estimator model  $f_p$  to fuse the logits of models

We adopt the self-perturbation [37] to train the weight estimator at the first stage. Agnostic to any of the attacks, a self-perturbation-trained model is able to distinguish images from benign and adversarial. Details of the self-perturbation are given in the supplementary.

The weight estimator  $f_p$  outputs a weight vector  $\mathbf{w} \in \mathbb{R}^2$  to ensemble the defense model and the target model:

$$\text{logit}_i(\mathbf{x}) = \mathbf{w} \cdot [f_t(\mathbf{x}), f_i(\mathbf{x})]^\top \quad (10)$$

In this way, both the clean images and the adversarial images are correctly classified.

The overall algorithm of CAD framework is presented in Algorithm 1.

---

**Algorithm 1** Continual Adversarial Defense
 

---

**Input:** Benign dataset  $\mathcal{D}_{\text{train}}$ , initial attack  $A_0$ , target model  $f_t$ , and few-shot feedback  $\mathcal{A}_{\text{train},K}^i$  generated by attack  $A_i$  in stage  $i = 1, \dots, T$ .

**Output:** Defense model ensemble.

- 1: Generate initial adversarial dataset  $\mathcal{A}_{\text{train}}^0$  using  $A_0$ .
  - 2: Train weight estimator  $f_p$  on  $\mathcal{D}_{\text{train}}$  using self-perturbation.
  - 3: Rewrite the ground-truth of  $\mathcal{A}_{\text{train}}^i$  using Eq. (1).
  - 4: Optimize defense model  $f_0$  on  $\mathcal{A}_{\text{train}}^0$  using Eq. (5).
  - 5: Generate prototypes of  $A_0$  using Eq. (8) and add them to prototype set  $P_e$ .
  - 6: **for**  $i$  **in**  $1, \dots, T$  **do**
  - 7:   Fine-tune the part of the classifier preserved for the new attack using Eq. (9).
  - 8:   Generate prototypes of  $A_i$  using Eq. (8) and add them to prototype set  $P_e$ .
  - 9:   Ensemble the defense model  $f_i$  and the target model  $f_t$  using Eq. (15).
  - 10: **end for**
- 

## 5 Experiment

To validate the performance of CAD against various adversarial attack methods in the dynamic scenario, we conduct extensive empirical studies on two datasets and compare CAD to baselines from three research streams. For evaluation and analysis, we use two metrics in this section: (1) Classification accuracy against each attack after adaptation for defense performance evaluation. (2) Average accuracy of all attacks occurring within and before each stage, i.e. average incremental accuracy [27], for assessing the knowledge retention of the model.

**Datasets** CIFAR-10 [17] is a widely used dataset for adversarial attack and defense, containing 5000 images for training and 1000 images for testing in each of the 10 classes. ImageNet-100 [33] is a subset of ImageNet [4] and contains 100 classes with 1000 images for training and 100 images for testing in each class. Images from CIFAR-10 and ImageNet-100 are resized to  $32 \times 32$  and  $224 \times 224$  respectively. Before training, the above datasets endured data augmentation including horizontal flip and random crop.

**Attack Algorithms** We choose PGD- $l_\infty$  [23] as the initial attack. After that, we select 8 adversarial attack methods under  $l_\infty$ : BIM [18], RFGSM [34], MIM [6], DIM [40], NIM [21], SNIM [21], VNIM [38] and VMIM [38] to compose the attack pool in defense performance evaluation. The perturbation magnitude of these attacks is set to  $\epsilon = 8/255$  for CIFAR-10 and  $\epsilon = 4/255$  for ImageNet-100

following [44]. As for evaluating the capability of CAD in migrating catastrophic forgetting,  $l_\infty$  attack VMIM [38] and SNIM [21],  $l_2$  attack CW [1] and DeepFool [25],  $l_1$  attack EAD [2] and EADEN [2], and  $l_0$  attack OnePixel [31] and SparseFool [24] compose the attack pool. Details of attack parameters are given in the supplementary.

| Stage                        | 0           | 1           | 2           | 3           | 4           | 5           | 6           | 7           | 8           | -           |
|------------------------------|-------------|-------------|-------------|-------------|-------------|-------------|-------------|-------------|-------------|-------------|
| Attack                       | PGD         | SNIM        | BIM         | RFSGM       | MIM         | DIM         | NIM         | VNIM        | VMIM        | Clean       |
| None-defense                 | 0.6         | 1.3         | 0.0         | 0.0         | 0.0         | 0.0         | 0.2         | 0.0         | 0.0         | <b>96.4</b> |
| TRADES [44]                  | 55.8        | 60.2        | 57.4        | 55.9        | 55.8        | 57.1        | 57.1        | 58.9        | 57.3        | 84.8        |
| JEM [10]                     | 55.8        | 62.0        | 46.5        | 52.3        | 52.4        | 51.1        | 51.4        | 57.0        | 48.2        | 91.7        |
| PAT [19]                     | 45.5        | 45.1        | 43.8        | 45.5        | 45.3        | 45.2        | 45.2        | 43.9        | 45.4        | 69.3        |
| GAIRAT [45]                  | 66.9        | 70.4        | 66.4        | 66.9        | 66.7        | 66.5        | 66.5        | 68.6        | 66.4        | 89.4        |
| FastAdv [14]                 | 37.1        | 39.6        | 36.8        | 37.0        | 37.7        | 37.7        | 54.6        | 36.4        | 37.6        | 75.2        |
| RPF [5]                      | 60.9        | 52.8        | 52.2        | 58.9        | 54.9        | 57.6        | 57.5        | 53.5        | 52.6        | 83.5        |
| DMAT [39]                    | 71.7        | 76.0        | 73.1        | 71.7        | 71.7        | 73.0        | 73.0        | 75.5        | 73.0        | 92.4        |
| EBM [12]                     | 75.2        | 72.9        | 73.0        | 76.6        | 76.5        | 72.4        | 73.9        | 74.0        | 73.8        | 86.8        |
| ADP [41]                     | 85.4        | 80.5        | 79.3        | 84.4        | 85.1        | 84.1        | 83.7        | 81.0        | 79.1        | 80.5        |
| DiffPure [26]                | 72.5        | 70.2        | 69.8        | 70.1        | 72.2        | 73.4        | 73.5        | 72.7        | 69.4        | 89.3        |
| <b>CAD(ours)</b>             | <b>94.5</b> | <b>95.4</b> | <b>93.4</b> | <b>94.7</b> | <b>95.0</b> | <b>93.7</b> | <b>93.7</b> | <b>95.2</b> | <b>93.7</b> | 95.8        |
| <b>CAD<sup>†</sup>(ours)</b> | <b>94.4</b> | <b>95.5</b> | <b>95.6</b> | <b>94.1</b> | <b>94.6</b> | <b>94.3</b> | <b>95.1</b> | <b>95.1</b> | <b>95.7</b> | <b>96.0</b> |

**Table 1:** Classification accuracy(%) against various attacks( $l_\infty$ ) on CIFAR-10. Volumn "Clean" represents the standard accuracy of clean images. **CAD<sup>†</sup>** denotes premium-CAD that is not constrained by efficient memory and few-shot defense feedback.

**Implementation Details** Both the target model and defense model use ResNet as the backbone network in our method. Specifically, we use WideResNet-28-10 [42] for CIFAR-10 following [10] and ResNet-50 [11] for ImageNet-100 following [19]. A 4-layer ConvNet is used as the weight estimator model. The cosine classifier [8] is adopted as the classifier of the defense model. We utilize Torchattacks [15] for generating adversarial images. The amount of feedback per class is set to  $K = 10$ . The number of stages is set to  $T = 8$  since there are 9 attacks (PGD is the initial attack). Parameters of Beta distribution are set to  $\alpha = \beta = 2$  and the trade-off parameter for  $\mathcal{L}_0$  is set to  $\gamma = 0.01$  following [47]. Epochs for training  $f_0$  are set to 100 and fine-tuning epochs are set to 4.

**Defense Baselines** We first compare to adversarial training methods TRADES [44], JEM [10], GAIRAT [45], FastAdv [14], RPF [5] and DMAT [39], and purification methods EBM [12], ADP [41] and DiffPure [26] in defense performance evaluation. As for evaluating the capability of CAD in migrating catastrophic forgetting, we compare to CL methods EWC [16], SSRE [51], BEEF [36], and FACT [47]. Besides, we propose another variant of our method denoted as premium-CAD in the case of no constraint of memory and no concerns about the amount of feedback. In premium-CAD, we train additional attack-specific defense models using abundant feedback in each stage, and ensemble them with the target model by the weight estimator. Details about the implementation of defense baseline and premium-CAD are given in the supplementary.

### 5.1 Comparisons to Baselines

To evaluate the defense performance, we first compared CAD to defense baseline methods in defending against 9 adversarial attacks. For CAD, the defense environment is dynamic, with attacks occurring at different stages. The other baseline methods operate in a static defense environment that does not differentiate the order of attacks. All the evaluation is conducted on the whole test set of CIFAR-10 and ImageNet-100. Classification accuracy is reported in Tab. 1 and Tab. 2.

| Stage                        | 0           | 1           | 2           | 3           | 4           | 5           | 6           | 7           | 8           | -           |
|------------------------------|-------------|-------------|-------------|-------------|-------------|-------------|-------------|-------------|-------------|-------------|
| Attack                       | PGD         | SNIM        | BIM         | RFGSM       | MIM         | DIM         | NIM         | VNIM        | VMIM        | Clean       |
| None-defense                 | 0.2         | 0.0         | 0.0         | 0.0         | 0.0         | 0.0         | 0.1         | 0.0         | 0.0         | <b>89.8</b> |
| TRADES [44]                  | 46.5        | 45.5        | 49.6        | 46.2        | 48.0        | 47.7        | 46.7        | 48.2        | 49.5        | 76.2        |
| GAIRAT [45]                  | 59.8        | 60.2        | 58.4        | 59.2        | 58.8        | 58.9        | 58.9        | 59.7        | 59.8        | 74.1        |
| RPF [5]                      | 56.4        | 49.9        | 51.3        | 56.6        | 54.4        | 52.6        | 53.9        | 53.3        | 50.1        | 69.4        |
| DMAT [39]                    | 64.3        | 65.1        | 66.2        | 65.9        | 65.4        | 64.4        | 64.1        | 65.8        | 65.6        | 75.9        |
| ADP [41]                     | 77.2        | 76.9        | 71.8        | 71.8        | 75.6        | 75.9        | 76.2        | 76.0        | 72.3        | 74.1        |
| DiffPure [26]                | 53.2        | 53.0        | 52.4        | 55.8        | 53.9        | 53.4        | 52.6        | 54.7        | 52.3        | 73.6        |
| <b>CAD(ours)</b>             | <b>83.7</b> | <b>83.4</b> | <b>82.0</b> | <b>82.5</b> | <b>83.5</b> | <b>82.0</b> | <b>81.9</b> | <b>82.2</b> | <b>81.9</b> | <b>88.1</b> |
| <b>CAD<sup>†</sup>(ours)</b> | <b>83.5</b> | <b>83.9</b> | <b>84.0</b> | <b>82.6</b> | <b>84.3</b> | <b>83.8</b> | <b>84.2</b> | <b>82.2</b> | <b>81.4</b> | 87.8        |

**Table 2:** Classification accuracy(%) against various attacks( $l_\infty$ ) on ImageNet-100.

| Stage                        | 0           | 1           | 2           | 3           | 4           | 5           | 6           | 7           | 8           |
|------------------------------|-------------|-------------|-------------|-------------|-------------|-------------|-------------|-------------|-------------|
| Attack                       | PGD         | SNIM        | VNIM        | CW          | DeepF.      | EAD         | EADEN       | OnePixel    | SparseF.    |
| None-defense                 | 0.6         | 1.3         | 0.0         | 0.0         | 8.6         | 0.0         | 0.2         | 39.1        | 29.7        |
| EWC [16]                     | <b>95.5</b> | 68.2        | 67.0        | 23.7        | 23.6        | 23.7        | 26.9        | 25.9        | 22.2        |
| SSRE [51]                    | 89.1        | 82.5        | 78.1        | 65.8        | 58.4        | 50.6        | 47.5        | 42.4        | 37.8        |
| BEEF [36]                    | 94.9        | 83.1        | 84.7        | 82.3        | 77.9        | 74.2        | 73.8        | 72.6        | 64.5        |
| FACT [47]                    | 94.5        | 87.2        | 86.4        | 81.5        | 80.9        | 78.6        | 78.4        | 78.2        | 74.6        |
| <b>CAD(ours)</b>             | <b>94.5</b> | <b>89.1</b> | <b>90.5</b> | <b>84.1</b> | <b>84.8</b> | <b>81.1</b> | <b>82.1</b> | <b>82.8</b> | <b>78.2</b> |
| <b>CAD<sup>†</sup>(ours)</b> | 94.4        | <b>95.5</b> | <b>95.1</b> | <b>95.2</b> | <b>94.9</b> | <b>95.3</b> | <b>94.6</b> | <b>96.0</b> | <b>95.2</b> |

**Table 3:** Continual defense performance (Average incremental accuracy(%)) against attacks under different norms  $l_{p=0,1,2,\infty}$  on CIFAR-10. DeepF. and SparseF. denote DeepFool [25] and SparseFool [24] respectively.

As depicted in Tab. 1 and Tab. 2, despite the small scale of feedback, both CAD and premium-CAD demonstrate strong adaptability to each type of attack. When compared with the top baseline methods DMAT [39] and ADP [41], CAD outperforms them by approximately 10% on CIFAR-10 and 6% on ImageNet-100 for each attack. This underscores its capacity for continuous adaptation in response to emerging attacks. Another notable advantage of CAD is its ability to maintain high classification performance for clean images, achieving 95.8% accuracy on CIFAR-10 and 88.1% on ImageNet-100, while the target model stands at 96.4% on CIFAR-10 and 89.8% on ImageNet-100. This can be attributed to the generic representation learned by the weight estimator for adversarial examples, enabling it to effectively differentiate between clean and adversarial images.

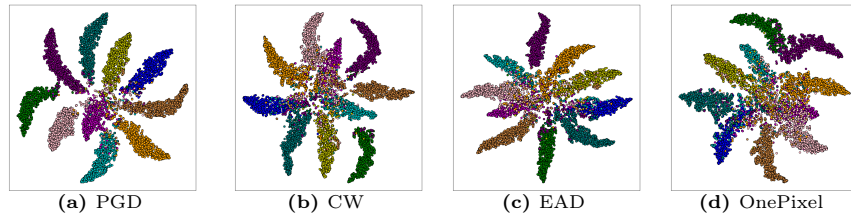


**Fig. 3:** T-SNE diagrams of features extracted from adversarial test data encoded by the defense model after all stages. Each color represents a class of CIFAR10. After several steps of adaptation, CAD retains the capability to categorize the attacked data.

To assess the effectiveness of CAD in retaining knowledge, we compare it to CL baseline methods through experiments on CIFAR-10 with attacks under different norms  $l_{p=0,1,2,\infty}$ . All baseline methods are functioned within our dynamic scenario. As depicted in Tab. 3, both CAD and premium-CAD maintain robust defense performance despite changes in attack types. However, as the variety of attack types increases, the defense performance gradually diminishes. This indicates that defending against an expanding array of attack types presents a more challenging task for continual defense. Compared with the top baseline method FACT [47], CAD consistently outperforms it by an average of approximately 3.4%, highlighting CAD’s effectiveness in mitigating catastrophic forgetting.

It is noteworthy that premium-CAD surpasses all baseline methods. Given sufficient defense feedback and memory resources, premium-CAD emerges as the superior choice.

## 5.2 Ablation Study

As argued, embedding reservation facilitates easier adaptation of the defense model and mitigates overfitting. Prototype augmentation preserves the decision boundary of previous stages, while model ensemble ensures robust classification performance for both clean and adversarial images. Therefore, we proceed to conduct an ablation study using 4 attacks PGD( $l_\infty$ ), CW( $l_2$ ), EAD( $l_1$ ), and

| Stage                    | 0           | 1           | 2           | 3           | -           |
|--------------------------|-------------|-------------|-------------|-------------|-------------|
| Attack                   | PGD         | CW          | EAD         | OnePixel    | Clean       |
| w/o $L_{\text{virtual}}$ | 94.5        | 82.4        | 76.1        | 71.8        | 95.8        |
| w/o $L_{\text{proto}}$   | 94.4        | 89.5        | 80.0        | 78.5        | 95.8        |
| w/o $f_p$                | 94.5        | 89.9        | 86.6        | 85.3        | 55.9        |
| <b>CAD(ours)</b>         | <b>94.5</b> | <b>89.9</b> | <b>86.6</b> | <b>85.3</b> | <b>95.8</b> |

**Table 4:** Average incremental accuracy(%) on CIFAR-10 for ablation.

Additionally, we provide T-SNE diagrams of features extracted from adversarial test data in Fig. 3 to visualize the defense capability of CAD after adaptation. These features are encoded by the defense model after the last stage of adapting to OnePixel attack. From (a) to (d) in Fig. 3, the clustering of features

OnePixel( $l_0$ ) to validate the efficacy of each component. As shown in Tab. 4, CAD without  $L_{\text{virtual}}$  and  $L_{\text{proto}}$  experiences a decrease of 13.5% and 6.8% respectively in the last stage. The absence of model ensemble leads to the inability to uphold performance on clean images.

becomes less and less discernible, indicating that the difficulty of few-shot adaptation increases with the introduction of new attack types. After adaptation, CAD maintains its defense performance against previous attacks, illustrating its ability to mitigate catastrophic forgetting as demanded in Principle 1.

### 5.3 Multiple Attacks in One Stage

In practice, it is common for multiple attacks to occur simultaneously within a

| Stage      | 0    | 1    | 2    | 3    |
|------------|------|------|------|------|
| number = 1 | 94.5 | 95.4 | 93.4 | 94.7 |
| number = 2 | 94.5 | 94.4 | 93.5 | 92.8 |
| number = 3 | 94.5 | 93.9 | 93.6 | 92.5 |

**Table 5:** Classification accuracy(%) about the number of attacks( $l_\infty$ ) in one stage against these attacks still remains at a high level: 92.8% and 92.5% at stage 3 respectively. The results indicate that CAD continues to perform effectively even when confronted with multiple simultaneous attacks.

### 5.4 Number of Shots for Adaptation

As indicated in Principle 2, the defense adaptation relies on few-shot defense feedback. To investigate the influence of the amount of feedback  $K$  per class, we

| Stage    | 0    | 1    | 2    | 3        |
|----------|------|------|------|----------|
| Attack   | PGD  | CW   | EAD  | OnePixel |
| $K = 15$ | 94.5 | 90.0 | 88.4 | 85.5     |
| $K = 10$ | 94.5 | 89.9 | 86.6 | 85.3     |
| $K = 5$  | 94.5 | 89.4 | 86.1 | 84.6     |
| $K = 1$  | 94.5 | 87.9 | 84.6 | 83.4     |

**Table 6:** Average incremental accuracy(%) with different feedback scale.

single stage. To assess CAD’s adaptability in such scenarios, we evaluate the classification accuracy when faced with 1, 2, and 3 concurrent attacks on CIFAR-10. As presented in Tab. 5, when the number of attacks increases to 2 and 3, the classification accuracy against these attacks still remains at a high level: 92.8% and 92.5% at stage 3 respectively. The results indicate that CAD continues to perform effectively even when confronted with multiple simultaneous attacks.

conducted tests with  $K = 15, 10, 5, 1$  on CIFAR-10. The results presented in Tab. 6 illustrate that defense performance diminishes as  $K$  decreases. Nevertheless, even with reduced  $K$ , CAD continues to efficiently defend against adversarial attacks (93.4% when  $K = 1$  at stage 3), highlighting its strong capability in few-shot scenarios.

### 5.5 Memory Allowance for Adaptation

As outlined in Principle 3, we need to employ memory efficiently for continual defense. In order to demonstrate CAD’s effectiveness in conserving memory, we conducted tests to measure the occupied memory space and model size at each

| Stage                  | Cache Size |       |        | Model Size |      |      |
|------------------------|------------|-------|--------|------------|------|------|
|                        | 1          | 2     | 3      | 1          | 2    | 3    |
| <b>CAD</b>             | 50.3K      | 75.5K | 100.4K | 141M       | 141M | 141M |
| <b>CAD<sup>†</sup></b> | 257M       | 377M  | 504M   | 280M       | 419M | 558M |

**Table 7:** Comparison of the Cache Size and Model Size (Byte) between CAD and premium-CAD.

stage on CIFAR-10. As depicted in Tab. 7, CAD requires neither a large cache footprint (with only a 25KB growth per stage) nor an expansion of the model size. This underscores our approach’s ability to utilize efficient memory.

## 6 Conclusion

The operational environment for defense systems is inherently dynamic, making it unrealistic to expect any defense method to effectively address all types of attacks. In response to this challenge, we introduce the first Continual Adversarial Defense (CAD) framework. CAD is engineered to collect few-shot defense feedback from the Internet and dynamically adapt to a diverse range of attacks as they emerge in sequential stages. In consideration of practical applicability, we have formulated four principles including few-shot feedback and memory-efficient adaptation, and CAD demonstrates strong performance when operating under these principles. Through experiments conducted on CIFAR-10 and ImageNet-100, we have demonstrated the effectiveness of our approach in combating multiple stages of various adversarial attacks, achieving significant improvements over baseline methods.

## References

1. Carlini, N., Wagner, D.: Towards evaluating the robustness of neural networks. In: 2017 IEEE Symposium on Security and Privacy (SP). pp. 39–57. IEEE (2017) [11](#)
2. Chen, P.Y., Sharma, Y., Zhang, H., Yi, J., Hsieh, C.J.: Ead: elastic-net attacks to deep neural networks via adversarial examples. In: AAAI. vol. 32 (2018) [11](#)
3. Croce, F., Andriushchenko, M., Sehwag, V., Debenedetti, E., Flammarion, N., Chiang, M., Mittal, P., Hein, M.: Robustbench: a standardized adversarial robustness benchmark. In: Thirty-fifth Conference on Neural Information Processing Systems Datasets and Benchmarks Track (2021), <https://openreview.net/forum?id=SSKZPJct7B> [3](#)
4. Deng, J., Dong, W., Socher, R., Li, L.J., Li, K., Fei-Fei, L.: Imagenet: A large-scale hierarchical image database. In: CVPR (2009) [10](#)
5. Dong, M., Xu, C.: Adversarial robustness via random projection filters. In: CVPR. pp. 4077–4086 (2023) [11](#), [12](#)
6. Dong, Y., Liao, F., Pang, T., Su, H., Zhu, J., Hu, X., Li, J.: Boosting adversarial attacks with momentum. In: CVPR. pp. 9185–9193 (2018) [10](#)
7. Dong, Y., Pang, T., Su, H., Zhu, J.: Evading defenses to transferable adversarial examples by translation-invariant attacks. In: CVPR. pp. 4307–4316 (2019) [4](#)
8. Gidaris, S., Komodakis, N.: Dynamic few-shot visual learning without forgetting. In: CVPR. pp. 4367–4375 (2018) [11](#)
9. Goodfellow, I.J., Shlens, J., Szegedy, C.: Explaining and harnessing adversarial examples (2014) [4](#)
10. Grathwohl, W., Wang, K.C., Jacobsen, J.H., Duvenaud, D., Norouzi, M., Swersky, K.: Your classifier is secretly an energy based model and you should treat it like one. In: ICLR (2020) [4](#), [11](#)
11. He, K., Zhang, X., Ren, S., Sun, J.: Deep residual learning for image recognition. In: CVPR. pp. 770–778 (2016) [11](#)
12. Hill, M., Mitchell, J.C., Zhu, S.C.: Stochastic security: Adversarial defense using long-run dynamics of energy-based models. In: ICLR (2020) [4](#), [11](#)
13. Huang, H., Wang, Y., Chen, Z., Zhang, Y., Li, Y., Tang, Z., Chu, W., Chen, J., Lin, W., Ma, K.K.: Cmu-watermark: A cross-model universal adversarial watermark for combating deepfakes. In: AAAI. vol. 36, pp. 989–997 (2022) [2](#)

14. Jiang, Y., Liu, C., Huang, Z., Salzman, M., Susstrunk, S.: Towards stable and efficient adversarial training against  $l_1$  bounded adversarial attacks. In: ICML. pp. 15089–15104. PMLR (2023) [11](#)
15. Kim, H.: Torchattacks: A pytorch repository for adversarial attacks. arXiv preprint arXiv:2010.01950 (2020) [11](#), [3](#)
16. Kirkpatrick, J., Pascanu, R., Rabinowitz, N., Veness, J., Desjardins, G., Rusu, A.A., Milan, K., Quan, J., Ramalho, T., Grabska-Barwinska, A., et al.: Overcoming catastrophic forgetting in neural networks. *Proceedings of the national academy of sciences* **114**(13), 3521–3526 (2017) [11](#), [12](#)
17. Krizhevsky, A., Hinton, G., et al.: Learning multiple layers of features from tiny images. Technical report (2009) [10](#)
18. Kurakin, A., Goodfellow, I., Bengio, S.: Adversarial machine learning at scale (2016) [4](#), [10](#)
19. Laidlaw, C., Singla, S., Feizi, S.: Perceptual adversarial robustness: Defense against unseen threat models. In: ICLR (2020) [11](#)
20. Li, Y., Bai, S., Zhou, Y., Xie, C., Zhang, Z., Yuille, A.: Learning transferable adversarial examples via ghost networks. In: AAAI. vol. 34, pp. 11458–11465 (2020) [2](#)
21. Lin, J., Song, C., He, K., Wang, L., Hopcroft, J.E.: Nesterov accelerated gradient and scale invariance for adversarial attacks. In: ICLR (2019) [4](#), [10](#), [11](#)
22. Liu, Y., Li, Y., Schiele, B., Sun, Q.: Online hyperparameter optimization for class-incremental learning. In: AAAI (2022) [5](#), [7](#)
23. Madry, A., Makelov, A., Schmidt, L., Tsipras, D., Vladu, A.: Towards deep learning models resistant to adversarial attacks (2017) [4](#), [10](#)
24. Modas, A., Moosavi-Dezfooli, S.M., Frossard, P.: Sparsefool: a few pixels make a big difference. In: CVPR. pp. 9087–9096 (2019) [11](#), [12](#)
25. Moosavi-Dezfooli, S.M., Fawzi, A., Frossard, P.: Deepfool: a simple and accurate method to fool deep neural networks. In: Proceedings of the IEEE conference on computer vision and pattern recognition. pp. 2574–2582 (2016) [11](#), [12](#)
26. Nie, W., Guo, B., Huang, Y., Xiao, C., Vahdat, A., Anandkumar, A.: Diffusion models for adversarial purification. In: ICML (2022) [4](#), [11](#), [12](#)
27. Rebuffi, S.A., Kolesnikov, A., Sperl, G., Lampert, C.H.: icarl: Incremental classifier and representation learning. In: CVPR. pp. 2001–2010 (2017) [5](#), [7](#), [9](#), [10](#)
28. Salman, H., Sun, M., Yang, G., Kapoor, A., Kolter, J.Z.: Denoised smoothing: A provable defense for pretrained classifiers. *NeurIPS* **33**, 21945–21957 (2020) [4](#)
29. Shi, Y., Ling, H., Wu, L., Shen, J., Li, P.: Learning refined attribute-aligned network with attribute selection for person re-identification. *Neurocomputing* **402**, 124–133 (2020). <https://doi.org/https://doi.org/10.1016/j.neucom.2020.03.057>, <https://www.sciencedirect.com/science/article/pii/S0925231220304306> [2](#)
30. Snell, J., Swersky, K., Zemel, R.: Prototypical networks for few-shot learning. *NeurIPS* **30** (2017) [8](#), [9](#)
31. Su, J., Vargas, D.V., Sakurai, K.: One pixel attack for fooling deep neural networks. *IEEE Transactions on Evolutionary Computation* **23**(5), 828–841 (2019) [11](#), [3](#)
32. Taran, O., Rezaeifar, S., Holotyak, T., Voloshynovskiy, S.: Defending against adversarial attacks by randomized diversification. In: CVPR. pp. 11226–11233 (2019) [2](#), [4](#), [5](#)
33. Tian, Y., Krishnan, D., Isola, P.: Contrastive multiview coding. In: Computer Vision–ECCV 2020: 16th European Conference, Glasgow, UK, August 23–28, 2020, Proceedings, Part XI 16. pp. 776–794. Springer (2020) [10](#)



34. Tramèr, F., Kurakin, A., Papernot, N., Goodfellow, I., Boneh, D., McDaniel, P.: Ensemble adversarial training: Attacks and defenses. In: ICLR (2018) [9](#), [10](#)
35. Verma, V., Lamb, A., Beckham, C., Najafi, A., Mitliagkas, I., Lopez-Paz, D., Bengio, Y.: Manifold mixup: Better representations by interpolating hidden states. In: ICML. pp. 6438–6447 (2019) [8](#)
36. Wang, F.Y., Zhou, D.W., Liu, L., Ye, H.J., Bian, Y., Zhan, D.C., Zhao, P.: Beef: Bi-compatible class-incremental learning via energy-based expansion and fusion. In: ICLR (2022) [11](#), [12](#)
37. Wang, Q., Xian, Y., Ling, H., Zhang, J., Lin, X., Li, P., Chen, J., Yu, N.: Detecting adversarial faces using only real face self-perturbations. In: IJCAI. pp. 1488–1496 (8 2023). <https://doi.org/10.24963/ijcai.2023/165>, <https://doi.org/10.24963/ijcai.2023/165>, main Track [9](#), [1](#)
38. Wang, X., He, K.: Enhancing the transferability of adversarial attacks through variance tuning. In: CVPR. pp. 1924–1933 (2021) [4](#), [10](#), [11](#)
39. Wang, Z., Pang, T., Du, C., Lin, M., Liu, W., Yan, S.: Better diffusion models further improve adversarial training. In: ICML (2023) [4](#), [11](#), [12](#)
40. Wu, W., Su, Y., Lyu, M.R., King, I.: Improving the transferability of adversarial samples with adversarial transformations. In: CVPR. pp. 9020–9029 (2021) [4](#), [10](#)
41. Yoon, J., Hwang, S.J., Lee, J.: Adversarial purification with score-based generative models. In: ICML. pp. 12062–12072 (2021) [2](#), [4](#), [11](#), [12](#)
42. Zagoruyko, S., Komodakis, N.: Wide residual networks. arXiv preprint arXiv:1605.07146 (2016) [11](#)
43. Zhang, C., Song, N., Lin, G., Zheng, Y., Pan, P., Xu, Y.: Few-shot incremental learning with continually evolved classifiers. In: CVPR. pp. 12455–12464 (2021) [5](#), [8](#)
44. Zhang, H., Yu, Y., Jiao, J., Xing, E., El Ghaoui, L., Jordan, M.: Theoretically principled trade-off between robustness and accuracy. In: ICML. pp. 7472–7482 (2019) [2](#), [4](#), [11](#), [12](#), [3](#)
45. Zhang, J., Zhu, J., Niu, G., Han, B., Sugiyama, M., Kankanhalli, M.: Geometry-aware instance-reweighted adversarial training. In: ICLR (2020) [4](#), [11](#), [12](#)
46. Zhang, Z., Sabuncu, M.: Generalized cross entropy loss for training deep neural networks with noisy labels. In: Bengio, S., Wallach, H., Larochelle, H., Grauman, K., Cesa-Bianchi, N., Garnett, R. (eds.) NeurIPS. vol. 31 (2018) [8](#)
47. Zhou, D.W., Wang, F.Y., Ye, H.J., Ma, L., Pu, S., Zhan, D.C.: Forward compatible few-shot class-incremental learning. In: CVPR. pp. 9046–9056 (2022) [5](#), [8](#), [9](#), [11](#), [12](#), [13](#)
48. Zhou, D.W., Wang, F.Y., Ye, H.J., Zhan, D.C.: Pycil: a python toolbox for class-incremental learning. SCIENCE CHINA Information Sciences **66**(9), 197101–(2023). <https://doi.org/https://doi.org/10.1007/s11432-022-3600-y> [3](#)
49. Zhu, F., Cheng, Z., Zhang, X.y., Liu, C.l.: Class-incremental learning via dual augmentation. In: NeurIPS. vol. 34, pp. 14306–14318 (2021) [5](#)
50. Zhu, F., Zhang, X.Y., Wang, C., Yin, F., Liu, C.L.: Prototype augmentation and self-supervision for incremental learning. In: CVPR. pp. 5871–5880 (2021) [9](#)
51. Zhu, K., Zhai, W., Cao, Y., Luo, J., Zha, Z.J.: Self-sustaining representation expansion for non-exemplar class-incremental learning. In: CVPR. pp. 9296–9305 (2022) [5](#), [9](#), [11](#), [12](#)

## A Weight Estimator Base on Self-Perturbation

In CAD, we use clean images  $\mathcal{D}_{\text{train}}$  and self-perturbation [37] to train a weight estimator to ensemble the target model and the defense model. We craft half of the real images to pseudo adversarial images as negative samples and label other real images as positive samples. Then, we train a 4-layer ConvNet as the weight estimator  $f_p$  in a binary classification manner. In this section, we introduce the details of self-perturbation and model ensemble.

---

### Algorithm 2 Self-perturbation

---

**Input:** A empty perturbation matrix  $\boldsymbol{\eta}^p \in \mathbb{R}^{H \times W \times 3}$  with the same shape of real image  $\mathbf{x}^r$ .

**Parameter:** Max perturbation magnitude  $\epsilon$ , pattern mode.

**Output:** Self-perturbed image  $\mathbf{x}^p$ .

- 1: A random direction matrix  $R = \{\mathbf{r}_{ij}\} \in \mathbb{R}^{H \times W \times 3}$ .
- 2: **for**  $\boldsymbol{\eta}_{ij}$  **in**  $\boldsymbol{\eta}^p$  **do**
- 3:     Select random noise value  $\alpha$ .
- 4:     **if** pattern mode is ‘point-wise’ **then**
- 5:          $\boldsymbol{\eta}_{ij} := \alpha \cdot \mathbf{r}_{ij}$ .
- 6:     **else if** pattern mode is ‘block-wise’ **then**
- 7:         Select a random neighborhood  $A_{ij}$  of  $\boldsymbol{\eta}_{ij}$ .
- 8:         **for**  $\boldsymbol{\eta}_{ijk}$  **in**  $A_{ij}$  **do**
- 9:              $\boldsymbol{\eta}_{ijk} := \alpha \cdot \mathbf{r}_{ij}$ .
- 10:         **end for**
- 11:     **end if**
- 12: **end for**
- 13: Clip perturbation  $\boldsymbol{\eta}^p$  using Equation 11.
- 14: Generate self-perturbed image  $\mathbf{x}^p$  using Equation 12.
- 15: **return**  $\mathbf{x}^p$

---

*Self-Perturbation* As presented in Algorithm 2, we perturb each point in the point-wise pattern and each block in the block-wise pattern in a stochastic direction, where blocks are random neighborhoods of a set of scattered points. The generated perturbation image  $\boldsymbol{\eta}^p$  is constrained in  $l^\infty$  norm, and clipped according to  $\epsilon$ ,

$$\boldsymbol{\eta}^p = \text{Clip}_{[-\epsilon, \epsilon]}(\boldsymbol{\eta}^p). \quad (11)$$

A self-perturbed image is calculated as

$$\mathbf{x}^p = \mathbf{x}^r + \boldsymbol{\eta}^p. \quad (12)$$

*Model Ensemble* Trained with self-perturbation, the weight estimator  $f_p$  is able to distinguish between the clean and adversarial images. The output logit  $\mathbf{w}$  of  $f_p$  represents the probability of an image to be clean or adversarial. Therefore,

we use  $\mathbf{w}$  to ensemble the target model and the defense model:

$$\text{logit}_i(\mathbf{x}) = \mathbf{w} \cdot [f_t(\mathbf{x}), f_i(\mathbf{x})]^\top \quad (13)$$

In this way, both the clean images and the adversarial images are correctly classified.

## B Premium-CAD

We propose another variant of our method denoted as premium-CAD in the case of no constraint of memory and no concerns about the amount of feedback. In each stage, we train an attack-specific defense model using abundant feedback and ensemble the target model and all the defense models by a stage-evolved weight estimator.

*Attack-Specific Defense Model* In stage 0, the initial defense model is optimized under the full supervision using adversarial dataset  $\mathcal{A}_{\text{train}}^0 = \{(\mathbf{x}_{\text{adv}}^0, y) | \mathbf{x}_{\text{adv}}^0 = A_0(\mathbf{x}), (\mathbf{x}, y) \in \mathcal{D}_{\text{train}}\}$ . In stage  $i$ , another defense model is trained using abundant feedback  $\mathcal{A}_{\text{train}}^i = \{(\mathbf{x}_{\text{adv}}^i, y)\}_{N \times K}$  where  $N$  is the number of classes in dataset  $\mathcal{D}_{\text{train}}$  and  $K$  is the amount of feedback per class. The scale of feedback is set to  $K = 10$  in CAD and  $K = 1000$  in premium-CAD.

In this way, we have  $i + 1$  defense models in stage  $i$ . The defense model is designed to tackle adversarial examples from a specific attack, complementing each other.

---

### Algorithm 3 Premium Continual Adversarial Defense

---

**Input:** Benign dataset  $\mathcal{D}_{\text{train}}$ , abundant feedback  $\mathcal{A}_{\text{train}}^i$  generated by attack  $A_i$  for stage  $i = 1, \dots, T$ .

**Output:** Defense model ensemble.

- 1: **for**  $i$  **in**  $1, \dots, T$  **do**
  - 2:   Train an attack-specific defense model  $f_i$ .
  - 3:   Train a stage-evolved weight estimator  $f_p^i$ .
  - 4:   Ensemble the defense models  $[f_0, f_1, \dots, f_i]$  and the target model  $f_t$  using Eq. (15).
  - 5: **end for**
- 

*Stage-Evolved Weight Estimator* To ensemble the target model  $f_t$  and defense models  $[f_0, f_1, \dots, f_i]$ , we use a joint dataset  $\mathcal{D}_J^i = \bigcup_{j=0,1,\dots,i} \mathcal{A}_{\text{train}}^j \cup \mathcal{D}_{\text{train}}$  to train the weight estimator  $f_p^i$  in stage  $i$ . Feed an image to the weight estimator  $f_p^i$ , it output a weight vector  $\mathbf{w}^i \in \mathbb{R}^{i+2}$  to ensemble models:

$$\mathbf{w}^i = f_p^i(\mathbf{x}) \quad (14)$$

The final output for premium-CAD is:

$$\text{logit}_i(\mathbf{x}) = \mathbf{w}^i \cdot [f_t(\mathbf{x}), f_0(\mathbf{x}), f_1(\mathbf{x}), \dots, f_i(\mathbf{x})]^\top \quad (15)$$

The overall algorithm of premium-CAD framework is presented in Algorithm 3. The loss function for training attack-specific defense models and stage-evolved weight estimators is Cross-Entropy Loss.

## C Implementation Details

### C.1 Adversarial Attack

In this work, all of the adversarial attacks are implemented using TorchAttacks [15]. The perturbation magnitude of these attacks is set to  $\epsilon = 8/255$  for CIFAR-10 and  $\epsilon = 4/255$  for ImageNet-100 following [44]. Iterative steps and step size of iterative attacks are set to 10 and  $2/255$  respectively. The number of perturbed pixels of OnePixel [31] is set to 50. The other parameters are the default ones in TorchAttacks.

### C.2 Defense Baselines

The adversarial training baselines are implemented using RobustBench [3], while purification baselines are implemented using open-source code and model checkpoints. CL baselines are implemented using PyCIL [48]. The backbone models of both adversarial training methods and CL methods are standardized as WideResNet-28-10 for CIFAR-10 and ResNet-50 for ImageNet-100. CL models are trained under the same settings as CAD. Specifically, the training epochs and the amount of feedback per class for training CL models are set to 100 and  $K=10$ , respectively.